DNA-Electrochemical Biosensors: AFM Surface Characterisation and Application to Detection of *In Situ* Oxidative Damage to DNA

S. Carlos B. Oliveira and Ana Maria Oliveira-Brett*

Departamento de Química, Faculdade de Ciências e Tecnologia, Universidade de Coimbra, 3004-535 Coimbra, Portugal

Abstract: In recent years increased attention has been focused on the ways in which drugs interact with DNA, with the goal of understanding the toxic as well as chemotherapeutic effects of many molecules. The development of fast and accurate methods of DNA damage detection is important, especially caused by anticancer drugs or hazard compounds. The DNA-electrochemical biosensor is a very good model for evaluation of nucleic acid damage, and electrochemical detection a particularly sensitive and selective method for the investigation of specific interactions. The electrochemical sensor for detecting DNA damage consists of a glassy carbon electrode with DNA immobilized on its surface. The starting materials or the redox reaction products can be pre-concentrated on the dsDNA-biosensor surface, enabling electrochemical probing of the presence of short-lived radical intermediates and of their damage to dsDNA. AFM images were used to characterize different procedures for immobilization of nanoscale DNA surface films on carbon electrodes before and after interaction with hazard compounds. The electrochemical transduction is dynamic in that the electrode is itself a tuneable charged reagent as well as a detector of all surface phenomena, which greatly enlarges the electrochemical biosensing capabilities.

Keywords: DNA-electrochemical biosensor, DNA damage, carbon electrode, differential pulse voltammetry, DNA-anticancer drugs interaction.

1. INTRODUCTION

DNA is the intracellular target of most anticancer drugs which were developed to bind and interact strongly with DNA. These interactions cause changes in the structure of DNA and block the DNA replication machinery of tumour cells and eventually kill them. Consequently, the factors that determine affinity and selectivity in binding molecules to DNA need to be explained, because a quantitative understanding of the reasons that determine selection of DNA reaction sites is useful in designing sequence-specific DNA binding molecules for application in chemotherapy and in explaining the mechanism of action of anticancer drugs [1].

In recent years increased attention has been focused on the ways in which drugs interact with DNA, with the goal of understanding the toxic as well as chemotherapeutic effects of these small molecules [2]. Generally, there are two well-characterized binding modes for small molecules, including molecular drugs, with dsDNA: covalent (chemical modification of various DNA constituents) and non-covalent (outer electrostatic binding, groove binding, or intercalation) [3]. Intercalation and groove binding are the two most common modes by which small molecules bind directly and selectively to double-stranded DNA (dsDNA). Intercalation, which is an enthalpically driven process, results from deinsertion of a planar aromatic ring system between dsDNA base pairs with concomitant unwinding and lengthening of the DNA helix [4]. In contrast, groove binding, which is predominantly entropically driven, involves covalent and non-covalent (electrostatic) interactions that do not perturb the duplex structure to any great extent [5].

Anticancer drugs interact with DNA in many different ways. For one category of these DNA- anticancer drugs, the interaction with DNA is by means of chemical modification, guanine being the prime target. Another category binds to DNA to the double helix. This occurs either at the periphery or, in the case of some drugs, by means of intercalation between adjacent base-pairs [3, 6, 7].

Various methods with great sensitivity and specificity have helped to characterize the nature of the anticancer drug interaction with DNA, such as UV-VIS, IR and Raman spectroscopy, DNA footprinting, nuclear magnetic resonance, mass spectrometry, molecular modelling techniques, capillary electrophoresis, equilibrium dialysis, surface plasmon resonance, femtosecond laser spectroscopy, HPLC and electrochemistry [8].

Electrochemical techniques, such as pulse techniques, are suitable for studies of biological systems, for instance DNA-anticancer drugs interactions, since they are fast, low cost and have high sensitivity. One advantage of the use of pulse techniques is that they bring a great improvement in the signal-to-noise ratio compared to steady state techniques and, in many cases, greater selectivity [9].

The DNA-electrochemical biosensor, using differential pulse voltammetry, has been successfully used to investigate the interaction of anticancer drugs with DNA, and comparison with other methods shows greater sensitivity towards detecting small perturbations of the double-helical structure and the detection of DNA oxidative damage.

*Address correspondence to this author at the Departamento de Química, Faculdade de Ciências e Tecnologia, Universidade de Coimbra, 3004-535 Coimbra, Portugal; Tel: +351-239-852080; Fax: +351-239-827703;
E-mail: brett@ci.uc.pt

1386-2073/10 $55.00+.00 © 2010 Bentham Science Publishers Ltd.

Electrode surface modification has been done by different DNA adsorption immobilization procedures, electrostatic adsorption or evaporation, with the formation of a monolayer or a multilayer DNA film. A very important factor for the optimal construction of a DNA-electrochemical biosensor is the immobilization of the DNA probe on the electrode surface [10-13].

This review will focus specifically on the research that has been undertaken in the development of DNA-electrochemical biosensors, using a glassy carbon transducer substrate, and their application in the study of anticancer drug-DNA interactions. It will summarize and explain the different procedures used in the construction of DNA-electrochemical biosensors, the relevance of their surface AFM morphological characterization, as well as their application in order to obtain important information about the electron transfer anticancer drug mechanisms of action.

2. DNA STRUCTURES

In the development and design of DNA-electrochemical biosensors it is very important to know the DNA structure, the variations in DNA conformations – polymorphic - and to understand the electrochemical behavior of DNA molecules on the electrochemical transducer.

The double helical structure of DNA deduced by Watson and Crick [14] consists of two polynucleotide chains running in opposite directions and is made up of a large number of deoxyribonucleotides, each composed of a base, a sugar and a phosphate group. The bases are purines, guanine (G) and adenine (A), and pyrimidine, cytosine (C) and thymine (T) (Fig. **1**). The two chains of the double helix are held together by hydrogen bonds between purine and pyrimidine bases, and it is possible to identify a major and a minor groove, the latter with a higher negative density charge. The bases are always paired: adenine with thymine (A-T) and guanine with cytosine (G-C) and are on the inside of the helix, whereas the phosphate and deoxyribose units are on the outside. This double helical structure is stabilized by bound water that fits perfectly into the minor groove [3].

Nevertheless, the DNA structure can have more than one conformation in solution, depending on the pH and ionic environment. DNA double helices are classified either as A-DNA or B-DNA, the latter encompassing B-, C-, D-, E- and T-DNA, according to their conformations. Under physiological conditions, the dominant form is B-DNA. The rare A-DNA exists only in a dehydrated state, and although it has been shown that relatively dehydrated DNA fibers can adopt the A-conformation under physiological conditions, is still unclear whether DNA ever assumes this form *in vivo* [3].

Raman spectra studies revealed that a C-DNA form is produced at pH 4.0. The formation of C-DNA may be the result of an overall decrease in the charge of the polynucleotide chains; protonation permits closer approach of the phosphates [15-17]. In general, C-DNA resembles B-DNA, with conformation parameters of the nucleotide blocks changed only slightly [3].

The above are all right-handed double helices, but a left-handed conformation, Z-DNA, has also been discovered, adding considerable variation to the chameleon-like, adaptable character, of DNAs morphological structures in solution [3]. The most startling difference between Z-DNA and the other forms of DNA is the helical sense of the sugar-phosphate backbone. The backbone of Z-DNA adopts a left-handed turn, and when viewed from the side, the sugar-phosphate takes on a zigzag appearance as it winds along the outside of the molecule [18]. Z-type DNA exists *in vivo* and is the most different conformation from the normal B-DNA conformation.

Under conditions of extremes of pH or of heat the physical properties of dsDNA in solution change although no covalent bonds are broken: only the unwinding and separation of the double helical DNA structure occurs, a process referred to as denaturation. After denaturation, the

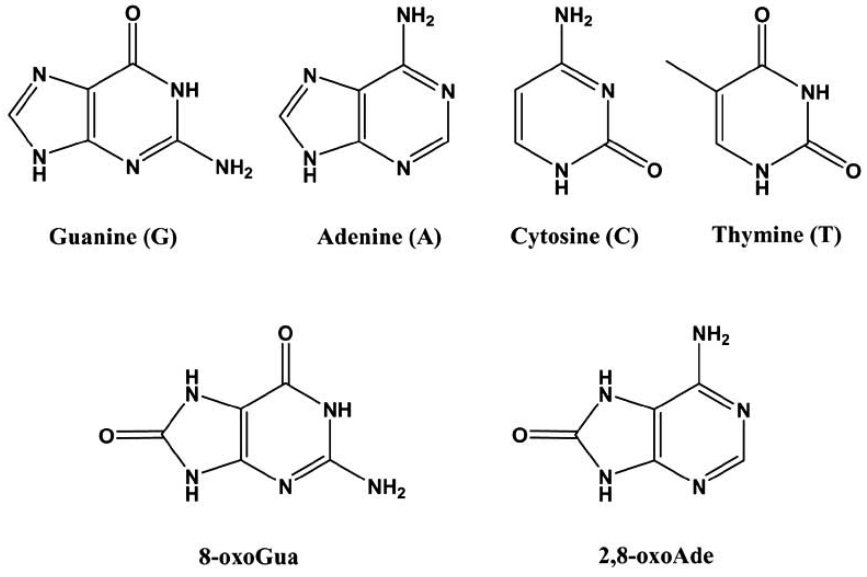

Fig. (1). Chemical structures: (G) guanine, (A) adenine, (C) cytosine, (T) thymine, (8-oxoGua) 8-oxoguanine and (2,8-oxoAde) 2,8-oxoadenine.

double-helix three-dimensional structure of DNA is disrupted into a random form called single-stranded DNA (ssDNA). Heat denaturation of dsDNA is called melting because the transition from dsDNA to ssDNA occurs over a narrow temperature range. In order to replicate and for RNA synthesis to occur, dsDNA must come apart, so the structures should not be too stable and, thus, denaturation is a physiological process. The reversible process is renaturation, also called annealing and hybridization, and corresponds to the reassociation or pairing of two complementary strands of DNA, a spontaneous process of great importance for achieving the biological functions of DNA.

3. ELECTROCHEMICAL OXIDATION OF DNA

The electrochemical behavior of DNA at different types of electrochemical transducers has been investigated for a number of years first using mercury electrodes [10, 19-24] and more recently solid electrodes, such as pyrolytic graphite electrodes [25, 26] and glassy carbon electrodes [27-30]. The reduction [10, 20] and oxidation [30] occur in the purine and pyrimidine bases, the sugar and phosphate groups being non-electroactive at carbon electrodes in aqueous solutions.

The electrochemical oxidation behavior of DNA free purine, guanine and adenine, and pyrimidine, cytosine and thymine, bases was studied at carbon electrodes in aqueous solutions [25, 26, 28-30]; they all present a pH-dependent electron transfer mechanism. The oxidation of purine bases occur at much lower positive potentials then that of the pyrimidine bases [30], which occurs at very high positive potentials, near the potential of oxygen evolution, and consequently their oxidation peaks are more difficult to detect. Equimolar mixtures of all four DNA bases, and also their nucleosides and nucleotides, have been quantified, at near physiological pH (Fig. **2**) [30]. The observed peak currents for pyrimidine bases are much smaller than those observed for the purine bases, meaning a slower oxidation reaction rate for the pyrimidine bases. Detection limits in the nanomolar range for purine bases and micromolar range for pyrimidine bases were obtained.

Results also showed that the purine and pyrimidine nucleosides and nucleotides are all electroactive on glassy carbon electrodes and that, for all four bases, the corresponding nucleosides and nucleotides are oxidized at potentials ~ 200 mV more positive than the free bases (Fig. **2A**) [30].

As the 2′-deoxyribose and the orthophosphate are not electroactive at glassy carbon electrodes in aqueous solutions and since the phosphate group appears to have no influence in the oxidation peak potential, the shift in the oxidation peak of nucleosides and nucleotides relative to the corresponding free bases is attributed to the stabilizing effect caused by the glycosidic bond on the π-system of purine and pyrimidine rings, making it more difficult to remove electrons from the bases. Also, the presence of the pentose phosphate group causes a significant decrease in the oxidation peak currents relative to the free base, being even lower for the nucleotide than for the nucleoside. The electrooxidation of the homopolynucleotides of all bases,

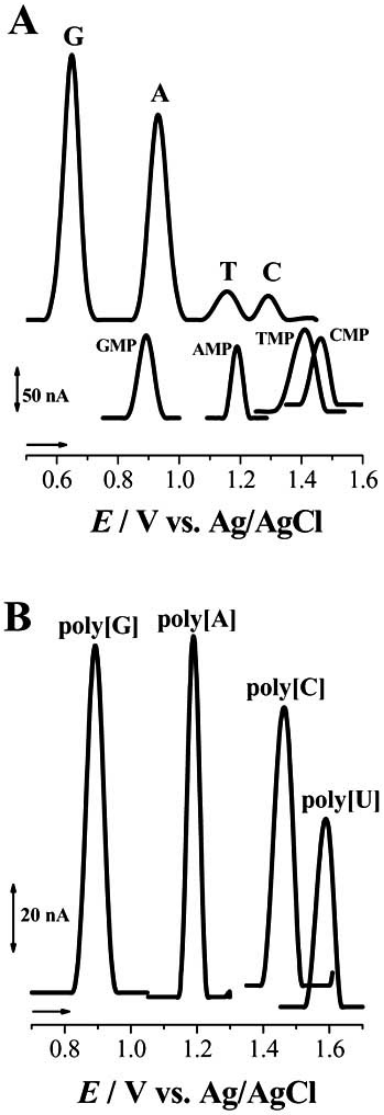

Fig. (2). Base line corrected differential pulse voltammograms: (**A**) for a 20 μM equimolar mixture of guanine (G), adenine (A), thymine (T) and cytosine (C), 20 μM guanosine-5-monophosphate (GMP), 20 μM adenosine-5-monophosphate (AMP), 500 μM thymidine-5-monophosphate (TMP) and 500 μM cytidine-5-monophosphate (CMP) in pH 7.4, 0.1 M phosphate supporting electrolyte with pre-conditioned a 1.5 mm diameter GCE and (**B**) for the following: 40 μg/mL poly[G] and poly[A], 100 μg/mL poly-[C], and 250 μg/mL poly[U] in pH 7.4, 0.05 M phosphate supporting electrolyte. Pulse amplitude 50 mV, pulse width 70 ms, scan rate 5 mV/s (From Ref. [30, 31] with permission).

namely poly[G], poly [A], poly [T], poly [C] and poly [U], has also been investigated [30, 31] and it was shown that they are oxidized at the same potential as the corresponding nucleotides (Fig. **2B**).

ssDNA has a single helix structure enabling the bases to be much more exposed in order to react at the electrode surface. The oxidation of ssDNA, at near physiological pH (Fig. **3A**) clearly shows the oxidation of the purine and pyrimidine residues (bases in the single helix), and after depurination, using mild acid conditions for 48 h, the peaks

for the free guanine and adenine bases appear (Fig. **3B**). Therefore, knowing that the nucleoside and nucleotide peak potentials are ~ 200 mV more positive than those of the free bases, it is easy to evaluate the integrity of the ssDNA using voltammetry [30].

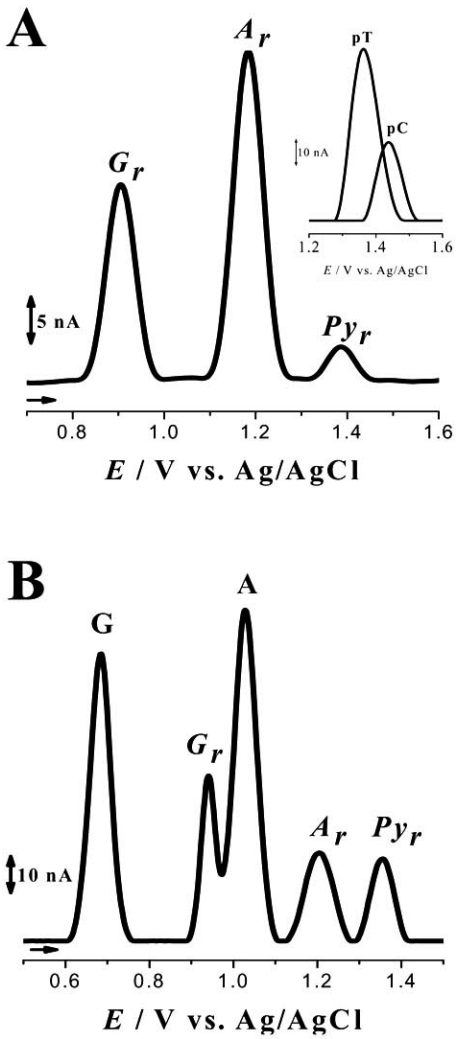

Fig. (3). Base line corrected differential pulse voltammogram obtained in a 40 µg/mL ssDNA solution pH 7.4 0.1 M phosphate supporting electrolyte with a pre-conditioned 1.5 mm diameter GCE. (**A**) G_r – guanine residue; A_r – adenine residue; Py_r – pyrimidine residue. Insert: Base line corrected differential pulse voltammograms obtained in a 100 µg/mL Poly[dT] (pT) and Poly[dC] (pC) solutions in pH 7.4, 0.1 M phosphate supporting electrolyte; (**B**) The ssDNA was allowed to undergo mild acid depurination during 48 hours prior to the experiment (see text for additional details). G – free guanine; A – free adenine; G_r – guanine residue; A_r – adenine residue; Py_r – pyrimidine residue in ssDNA. Pulse amplitude 50 mV, pulse width 70 ms, scan rate 5 mV s^{-1} (from ref. [30] with permission).

The electrooxidation of dsDNA at glassy carbon electrodes gives rise to two well-separated current peaks (Fig. **4B**) due to the oxidation of guanine and adenine residues (bases in the double helix), i.e. guanosine (dGuo) and adenosine (dAdo) groups [27, 32]. Due to the very low currents for the pyrimidine residues their peaks are not able to be detected. Also a large difference in the currents for dsDNA and ssDNA is observed, which is due to the different dsDNA and ssDNA structures. The difficulty in the transfer of electrons from the inside of the rigid double stranded form of DNA to the electrode surface is much greater than from the flexible single stranded form of DNA where the bases are in closer proximity to the electrode surface, leading to much higher peak currents in ssDNA (Fig. **4A**). The oxidation of the purine base oxidation products, 8-oxoGua or 2,8-oxoAde, is also shown in Fig. (**4B**).

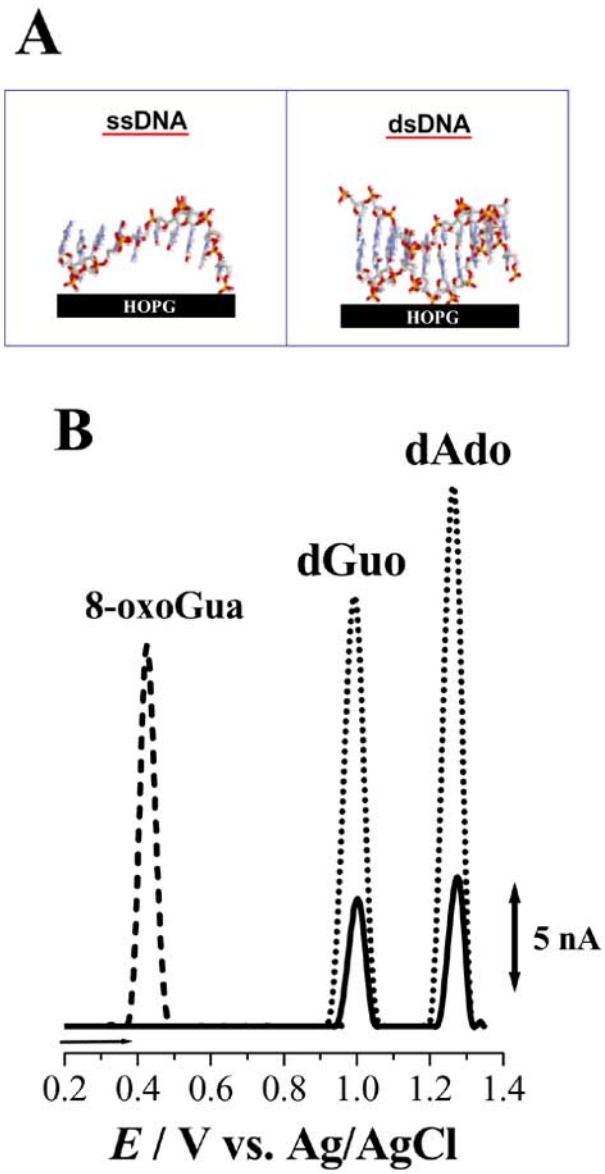

Fig. (4). (**A**) Schematic representation of the ssDNA and dsDNA immobilized on the carbon electrode and (**B**) baseline corrected differential pulse voltammograms of (▪▪▪) 5 µM 8-oxoG, (•••) 60 µg/mL ssDNA and (—) 60 µg/mL dsDNA in pH 4.5 0.1 M acetate buffer. Pulse amplitude 50 mV, pulse width 70 ms, scan rate 5 mV/s.

Care must be taken in always using excellent quality glassy carbon electrodes in the experiments because the properties of the glassy carbon surface, due to the impurities incorporated, vary significantly with the preparation procedure [9], and will affect the results obtained for the oxidation of DNA.

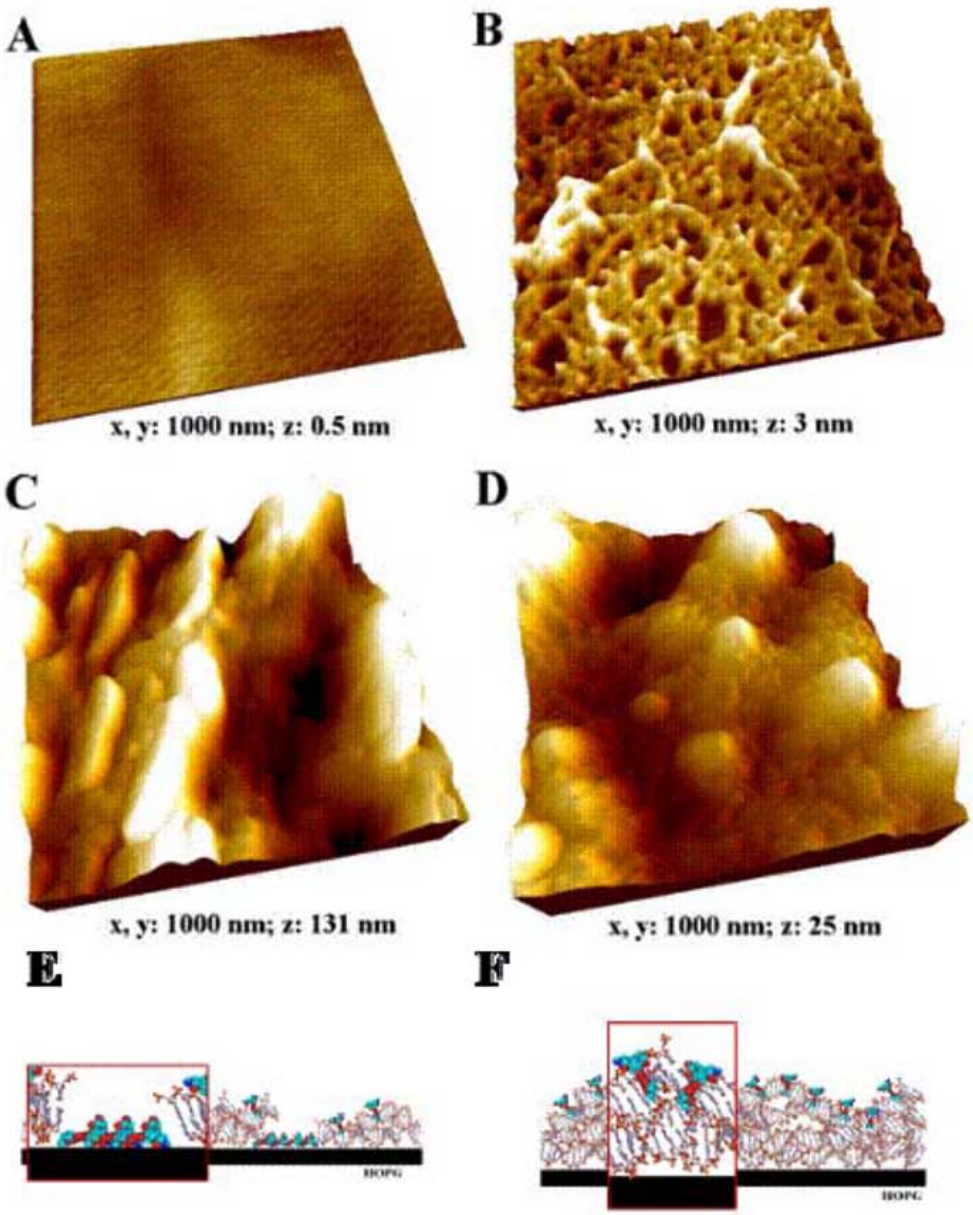

Fig. (5). MAC Mode AFM three-dimensional images in air of: (**A**) clean HOPG electrode; (**B**) thin layer dsDNA-biosensor surface, prepared onto HOPG by 3 min free adsorption from 60 μg/mL dsDNA in pH 4.5, 0.1 M acetate buffer; (**C**) multi-layer film dsDNA-biosensor, prepared onto HOPG by evaporation of 3 consecutive drops each containing 5 μL of 50 μg/mL dsDNA in pH 4.5, 0.1 M acetate buffer; (**D**) thick layer dsDNA-biosensor, prepared onto HOPG by evaporation from 37.5 mg/mL dsDNA in pH 4.5 0.1 M acetate buffer; (**E**, **F**) Schematic models of dsDNA-anticancer drugs interaction using (**E**) the thin layer and (**F**) the thick layer dsDNA-electrochemical biosensor (from ref. [12] with permission).

4. DNA-ELECTROCHEMICAL BIOSENSOR

A DNA-electrochemical biosensor is an integrated receptor-transducer device that uses DNA as a biomolecular recognition element to measure specific binding processes with DNA, through electrochemical transduction (Figs. **4**, **5**). Among the electrochemical transducers, carbon electrodes demonstrate several unique properties. The extensive potential window in the positive direction allows sensitive electrochemical detection of the oxidation peaks of the DNA nucleotides and, by monitoring the appearance of their oxidation products, of the oxidative damage caused to DNA by hazardous compounds.

The electrochemical transduction has the advantage in DNA-biosensor design of being rapid, sensitive, cost-effective and enable the *in situ* generation of reactive intermediates and detection of DNA damage. The electrooxidation signal of the components of DNA, such as nucleotides, nucleosides, purine and pyrimidine bases, can be employed as biological recognition elements for the determination of a more specific interaction (Figs. **2**, **3**). Different DNA-electrochemical biosensors can be prepared from known selected sequences of the DNA components, as in poly-homonucleotides and poly-heteronucleotides.

The electrical transduction of DNA damage is monitored by the changes of the response of the DNA-electrochemical

biosensor in the presence of the drug or hazard compound investigated, as the decrease and/or increase of the oxidation peak current of the DNA electroactive dGuo and dAdo groups, as the shifts of the formal potentials of the redox couple caused by the intercalation of nucleic acid-binding molecules into dsDNA and/or as the appearance of new electrochemical signals, such as those from 8-oxoGua or 2,8-oxoAde (Fig. **4**) It is also crucial for the correct interpretation of the results to know the electrooxidation behavior of the drug or hazard compound investigated alone in the same experimental conditions.

However, the performance, sensitivity and reliability of the DNA-electrochemical biosensor response are dictated by the correct procedure used in the DNA-electrochemical biosensor construction. The most important factor is the immobilization of the DNA probe on the electrode surface, usually done in the pH range 4.5 - 5.5 due to the better adsorption of DNA, on the carbon surface, consequently leading to an enhanced electrochemical response.

There are different procedures that can be followed in the DNA-electrochemical biosensor construction depending on the required application [12, 33]. Three procedures used in the DNA-electrochemical biosensor preparation by adsorption with or without applied potential, and their characterisation by AFM, are in Fig. (**5**):

1. *Thin-Layer dsDNA Biosensor*: prepared by immersing the GCE (d = 1.5 mm) surface in a 60 μg mL^{-1} dsDNA solution at + 0.30 V applied potential during 10 min (Fig. **5B**).
2. *Multi-Layer dsDNA Biosensor*: prepared by successively covering the GCE (d = 1.5 mm) surface with three drops of 5 μL each of 50 μg mL^{-1} dsDNA solution. After placing each drop on the electrode surface the biosensor is dried under a constant flux of N_2 (Fig. **5C**).
3. *Thick-Layer dsDNA Biosensor*: prepared by covering the GCE (d = 1.5 mm) surface with 10 μL of 35 mg mL^{-1} dsDNA solution and allowing it to dry in normal atmosphere (Fig. **5D**).

The thin dsDNA layer does not completely cover the HOPG electrode surface and the network structure has holes exposing the electrode underneath. The AFM image of a thin-layer dsDNA biosensor prepared on HOPG substrate is shown in Fig. (**5B**), showing that the dsDNA molecules adsorbed on the HOPG surface form a two-dimensional lattice with uniform coverage of the electrode. The DNA network patterns define nanoelectrode systems with different active surface areas on the graphite substrate, and form a biomaterial matrix to attach and study interactions with hazard molecules. The hazard molecules from the bulk solution will also diffuse and adsorb non-specifically on the electrode's uncovered regions. If the molecules are hydrophobic and with a high affinity with the carbon surface and also electroactive, two different contributions to the electrochemical signal, one from the adsorbed compound and the other due to the damage caused to immobilized DNA, will be obtained it being difficult to distinguish between them (Fig. **5E**).

Both the multi- and thick-layer dsDNA biosensor preparation give rise to complete coverage of the electrode surface, with regularly dispersed peaks and valleys as shown by AFM images (Fig. **5C**, **D**). The dsDNA-electrode surface interactions are stronger and these DNA layers are very stable on the HOPG surface. The big advantage of the dsDNA multi- and thick-layer DNA biosensors is that the electrode surface is completely covered by dsDNA and consequently the undesired binding of molecules to the electrode surface is not possible (Fig. **5F**). The advantage of the multi-layer dsDNA biosensor with respect to the thick-layer is the short time necessary for the multi-layer dsDNA biosensor construction.

5. AFM CHARACTERISATION OF THE dsDNA-ELECTROCHEMICAL BIOSENSOR SURFACE

The dsDNA-electrochemical biosensor consists of an electrode surface with deposited dsDNA. Considering the high oxidation potentials of the DNA bases a carbon electrode surface is the most appropriate, and glassy carbon or carbon paste are usually used as the electrode transducer substrate material for DNA immobilization.

These carbon electrode surfaces used for the voltammetric studies are very rough on the nanoscale and therefore unsuitable for AFM surface characterization. Highly oriented pyrolytic graphite (HOPG) is an atomically flat carbon electrode surface that has been used as substrate for AFM imaging (Fig. **5A**), and it is considered that the interactions between DNA and the different carbon surfaces, the adsorption and the degree of surface coverage, are very similar.

The adsorption of DNA at the liquid solid interface is affected by the nature of the solid surface (surface charge, no-polar – hydrophobic surface and polar – hydrophilic surface), the structure of DNA (single or double strand), and the characteristic of the liquid phase (pH, electrolyte concentration and temperature). A very good understanding of the adsorption and interactions of DNA with solid electrode surfaces is a major concern in DNA-electrochemical biosensor development, and information on the conformation of the adsorbed DNA, as well as the adsorption characteristics, is crucial for biosensor performance.

The DNA immobilization procedure, depending on the experimental conditions chosen, can lead to a partial (Fig. **5B**, **E**) or a total coverage (Fig. **5C**, **D**, **F**) of the carbon electrode surface. Total coverage of the carbon electrode surface ensures that the adsorption of undesired substances on the transducer surface does not occur (Fig. **5F**), and the dsDNA-electrochemical biosensor response is only due to the interaction of the analyte with dsDNA [34].

Extensive studies using atomic force microscopy (AFM) have been undertaken in order to clarify the adsorption behavior of DNA at carbon electrode surfaces [34-38]. The visualization of soft molecules, like DNA, weakly bound to the conducting surface of electrochemical transducers is better achieved using magnetic AC mode atomic force microscopy (MAC Mode AFM), which enables imaging the surface morphological structure of adsorbed nucleic acid and understanding the mechanism of adsorption and the nature of DNA-electrode surface interactions [34].

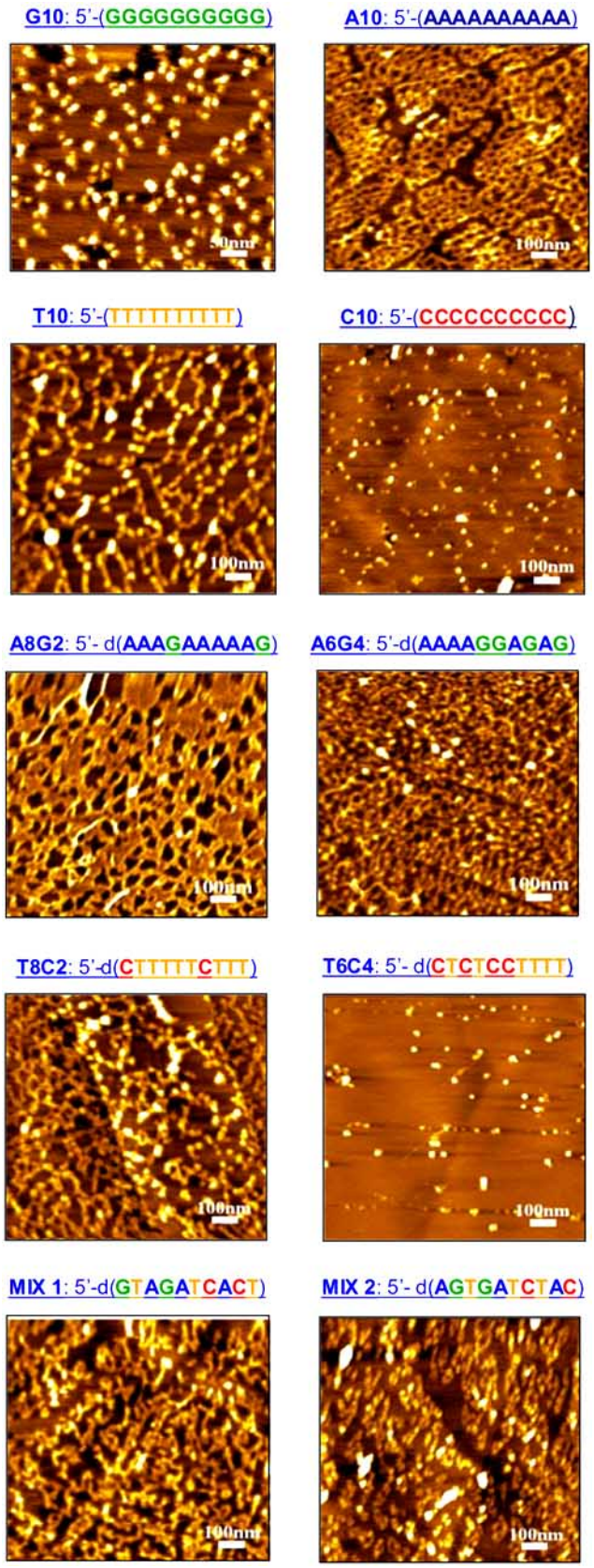

Fig. (6). MAC mode AFM topographical images in air of ODN molecules, immobilized by free adsorption during 3 min onto HOPG, from following 0.3 μM ODN solution in pH 4.5, 0.1 M acetate buffer (from ref. [38] with permission).

5.1. Adsorption of Homo- and Hetero-Oligonucleotides

The adsorption process of synthetic 10-mer homo- and hetero-oligodeoxynucleotides (10-mer ODNs) of known base sequences adsorbed spontaneously on the HOPG surface was investigated using AFM in order to better understand the mechanism of interaction of nucleic acids with the HOPG surface [38] (Fig. **6**). AFM images in air showed different adsorption patterns and degree of HOPG surface coverage for the ODNs, and correlation with the individual structure and base sequence of each ODN molecule. The ODNs interacted differently with the HOPG surface, according to the ODN sequence hydrophobic characteristics, being directly dependent on the molecular mass, the hydrophobic character of the individual bases and on the secondary structure of the molecule (Fig. **6**).

The different adsorption isotherms of the purine and pyrimidine bases at the graphite-water interface have been previously described in the literature [39] and the adsorption behavior followed the hydrophobicity series of the bases: G > A > T > C, resulting from the existence of two aromatic rings in the case of the purines. In the case of G10 sequences, guanines have the ability to stack upon each other to form four-stranded structures with a guanine tetrad core, and many G10 molecules form G-quartets morphology in solution [38].

The hydrophobic interactions with the HOPG hydrophobic surface explain the main adsorption mechanism, although other effects such as electrostatic and van der Waals interactions may contribute to the spontaneous adsorption process. The importance of the type of base existent at the ODN chain extremities on the adsorption process was investigated and different adsorption patterns were obtained with ODN sequences composed by the same group of bases aligned in a different order [38].

5.2. Adsorption of dsDNA and ssDNA

The adsorption of dsDNA on the HOPG hydrophobic surface has shown, using MAC Mode AFM, the influence of each DNA component, purine and pyrimidine bases, sugar and phosphate groups [12, 13]. The dsDNA adsorption is very dependent on the negatively charged DNA structure of a hydrophilic polyanion. Consequently, since all DNA bases (hydrophobic part) are on the inside of the helix their immobilization by spontaneous adsorption on the hydrophobic HOPG surface involves weak hydrophilic-hydrophobic interactions.

Detailed observations showed that immobilization by spontaneous adsorption process of DNA on HOPG leads to the formation of a nanoscale DNA-film with pores exposing the HOPG substrate surface (Fig. **7**). The influence of pH on the nanoscale DNA-film showed that the thin films formed in pH 5.3 acetate buffer always presented a better coverage of the HOPG surface with dsDNA molecules than thin films formed in pH 7.0 phosphate buffer. This is due to the dsDNA protonation in acetate buffer which neutralizes, in part, the phosphate groups and consequently increases their hydrophobicity and adsorbability on the hydrophobic HOPG surface (Fig. **7A**). On the other hand, at physiological pH, the dsDNA phosphate groups are fully or quasi-fully ionized (deprotonated) [3] which increases their hydrophilicity to

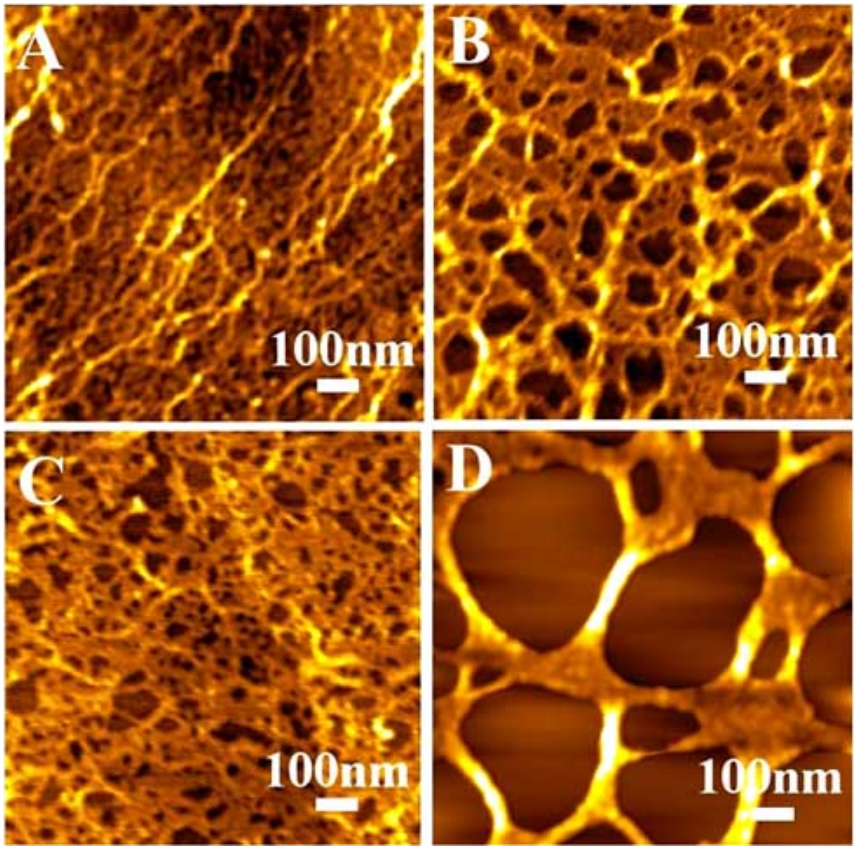

Fig. (7). MAC mode AFM topographical images in air of DNA molecules immobilized onto HOPG after 3 min in 60 μg/mL dsDNA; (**A**, **B**) free adsorption in (**A**) pH 5.3, 0.1 M acetate buffer and (**B**) pH 7.0, 0.1 M phosphate buffer; (**C**, **D**) at a deposition potential of +300 mV (*vs* AgQRE) in (**C**) pH 5.3 0.1 M acetate buffer and (**D**) pH 7.0 0.1 M phosphate buffer (From Ref. [34] with permission).

almost 100% and consequently decreases the adsorbability on the HOPG surface (Fig. **7B**).

Adsorption of dsDNA on the HOPG surface at an applied potential of + 300 mV, where no electron transfer reaction of the DNA components occurs, as was shown in Figs. (**2-4**), leads to a much stronger immobilization, enhancing the robustness and stability of the dsDNA nano-films with the formation of bigger network holes and a more condensed and compact self-assembled DNA lattice. This was characterized by MAC mode AFM [34] (Fig. **7C**, **D**).

In ssDNA the bases are more exposed to the solution, which facilitates the interaction of the hydrophobic aromatic rings of the purines and pyrimidines with the hydrophobic substrate. Consequently, ssDNA interacts and adsorbs much more strongly to the HOPG surface, when compared with dsDNA for the same solution concentration [34].

5.3. Adsorption of RNA

Similar to dsDNA, RNA is a highly negative charged hydrophilic molecule but RNA molecules also have the ability to catalyze chemical reactions, in mechanisms by which these so-called ribozymes accelerate chemical reactions. Anodic voltammetry of a small highly structured ribozyme showed that all four nucleobases (Fig. **8A**) could be detected on glassy carbon electrodes, and no signals corresponding to free nucleobases were found, indicating the integrity of the ribozyme molecules (Fig. **8B**), and this ribozyme spontaneously self-assembles uniformly in two-dimensional lattices on the HOPG surface as shown by AFM [31] (Fig. **8C**, **D**). Thus, AFM imaging and voltammetry enabled the monitoring of structural changes associated with RNA folding, binding, and catalysis.

6. ELECTROCHEMISTRY OF DNA BIOMARKERS FOR SENSING DNA DAMAGE

DNA damage is caused by hazard compounds or their metabolites and leads to multiple modifications in DNA, including DNA strand breaks, base-free sites and oxidized bases. Oxidative DNA damage caused for instance by oxygen-free radicals leads to multiple modifications in DNA, including base-free sites and oxidized bases that are potentially mutagenic [40, 41]. The major products of DNA oxidative damage are 8-oxo-7,8-dihydroguanine (8-oxoGua, 8-oxoguanine) which is the product of oxidation of guanine, the most easily oxidized base in DNA, and 2,8-dihydroxyadenine (2,8-oxoAde) [42] (Fig. **1**), and they can cause mutagenesis, hence the importance of screening for their occurrence.

The 8-oxoguanine mutagenicity causes loss of DNA base pairing specificity [42-44], and has been the subject of intensive research becoming widely accepted as a biomarker of oxidative DNA damage and cellular oxidative stress [45, 46]. Oxidative stress *in vivo* is an imbalance between prooxidant and antioxidant reactions which causes the disruption of the redox mechanisms. Elevated levels of

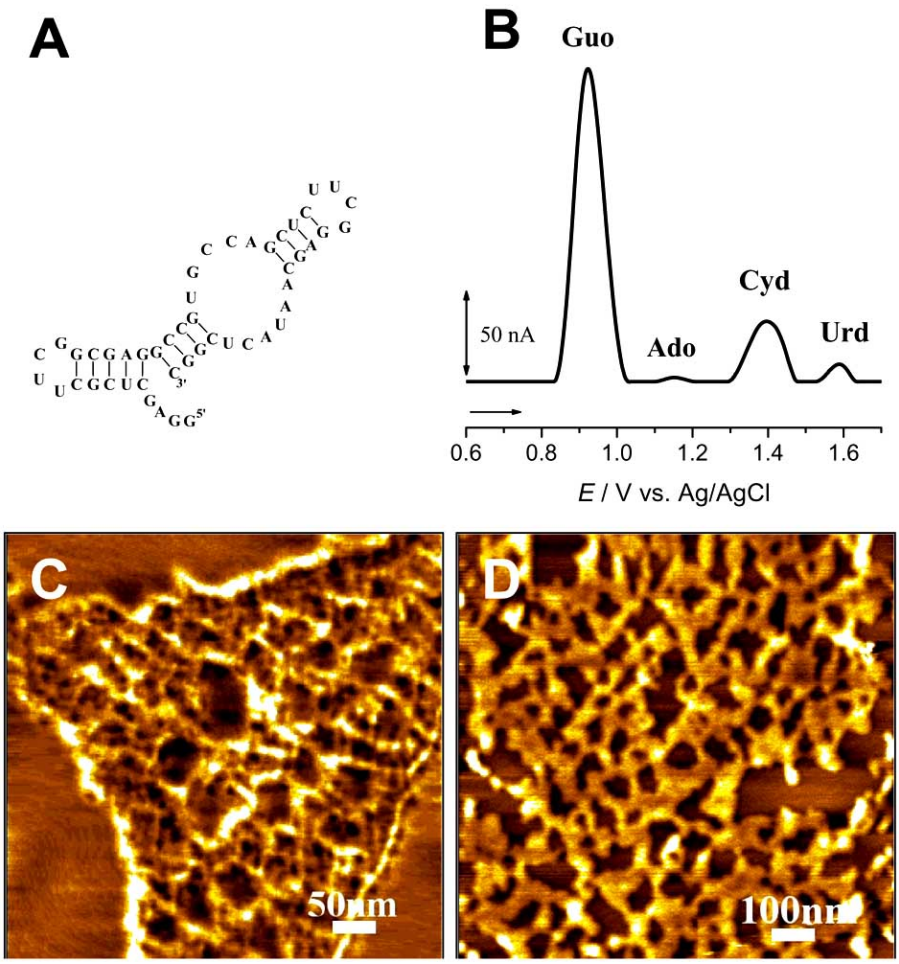

Fig. (8). (**A**) 49-Mer ribozyme secondary structure; (**B**) baseline-corrected differential pulse voltammograms obtained for 50 μg/mL 49-mer and (**C**, **D**) AFM topographical images in air of 49-mer ribozyme molecules immobilized by free adsorption during 3 min onto HOPG, from following: (**C**) 1 and (**D**) 5 μg/mL ribozymes in pH 7.1, 0.05 M phosphate buffer (From Ref. [31] with permission).

8-oxodGua were found in the urine and lung tissues of smokers [47] as well as in body fluids and DNA from human tissues of patients with disorders such as cancer, atherosclerosis, chronic hepatitis, cystic fibrosis, diabetes, acquired immunodeficiency syndrome, neurodegenerative and age-related diseases [48].

The electroactivity of 8-oxoGua and of 2,8-oxoAde was investigated by voltammetry [49, 50] and their oxidation peaks were chosen to monitor DNA oxidative damage since the oxidation potentials are lower than the oxidation potentials of the respective bases, they are easily detectable electrochemically and there is no overlap with the electrochemical oxidation peaks related to DNA. The electrochemical detection of these biomarkers has been essential for investigating the electrochemical mechanisms of DNA oxidative damage using the DNA-electrochemical biosensor [51-58].

7. DNA-ELECTROCHEMICAL BIOSENSORS FOR *IN SITU* DETECTION OF DNA OXIDATIVE DAMAGE

In recent years there has been a growing interest in the investigations of DNA-drug interactions, and the development of a fast and accurate method for detection of DNA damage, especially from anticancer drugs used in cancer therapy or in the development of new antineoplasic drugs, because DNA-electrochemical biosensors are a very good model for simulating nucleic acid interactions and to clarify mechanisms of action.

The interaction with dsDNA of three anticancer drugs, adriamycin, imatinib and thalidomide, that was investigated using the dsDNA-electrochemical biosensor or evaluated directly in the solution by electrochemical techniques, is described below to exemplify how the DNA-electrochemical biosensors are appropriate for investigating the DNA damage. The damage to immobilised DNA causes the appearance of oxidation peaks from DNA guanine and adenine purine bases which should always be detected. In the case of occurrence of DNA oxidative damage the oxidation peaks from the biomarkers for oxidative damage, 8-oxoGua or 2,8-oxoAde, should be evaluated.

7.1. Adriamycin

Adriamycin (Fig. **9A**), is an antibiotic of the family of anthracyclines that strongly adsorbs irreversibly to surfaces, and with antitumor properties known for more than 30 years, but it causes great cardiotoxicity. Adriamycin intercalates

within the double helix DNA and can undergo a reaction beginning with the transfer of a single electron to the quinone portion of the adriamycin ring system, generating a free radical, which can interact with DNA *in situ* with the products of this interaction being retained in the DNA layer. *In situ* electrochemical detection of potential-dependent dsDNA oxidative damage caused by adriamycin, intercalated into DNA, was carried out using the DNA-electrochemical biosensor [51].

Adriamycin electroactive [51] functional groups (the oxidizable hydroquinone group in ring B, and the reducible quinone function in ring C) are intercalated between the base pairs in the dsDNA. The reducible quinone group in ring C protrudes slightly into the minor groove, and this enables *in situ* (*in helix*) generation of an adriamycin radical within the double helix [2]. Therefore, a redox reaction between adriamycin and guanine residues inside the double helix of DNA occurs, and 8-oxoGua, the main product of guanine oxidation, was detected using the thin layer dsDNA-biosensor (Fig. **9B**). The mechanistic pathway involving two electrons and two protons [49] depends on the chemical environment surrounding guanine.

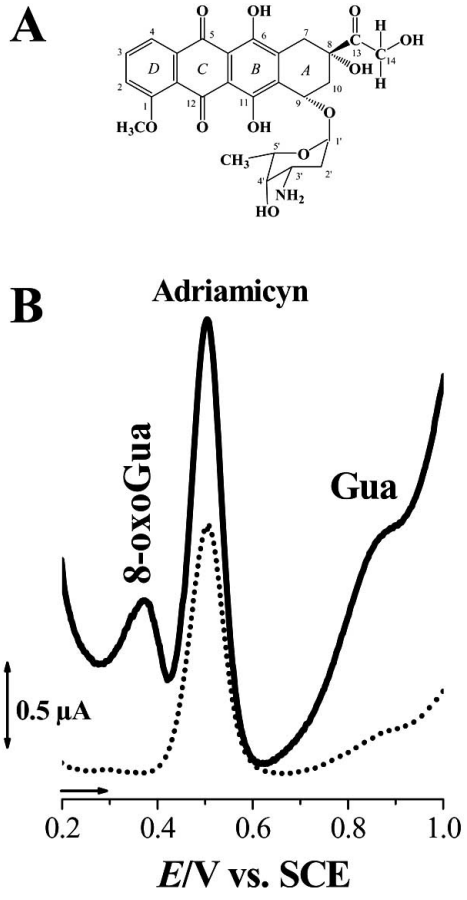

Fig. (9). (**A**) Chemical structure of adriamicyn and (**B**) differential pulse voltammograms in pH 4.5 0.1 M acetate buffer obtained with a thin layer dsDNA-modified GCE after being immersed in a 5 µM adriamyc in solution during 3 min and rinsed with water before the experiment in buffer: (•••) without applied potential; (—) applying a potential of - 0.6 V during 60 s. Pulse amplitude 50 mV, pulse width 70 ms, scan rate 5 mV/s. First scans (from ref. [52] with permission).

The thin layer dsDNA-biosensor was immersed during 3 min in an adriamycin solution, rinsed with water, and only afterwards transferred to buffer, where differential pulse voltammetry was performed. Results in acetate buffer (Fig. **9B**), showed different features. Without applying a negative potential only the peak for adriamycin oxidation at + 0.50 V occurs. After applying a potential of - 0.60 V during 60 s, the oxidation peak for guanine, and the oxidation peak for 8-oxoGua (Fig. **4**), also appeared. The reduced adriamycin radical, formed at – 0.60 V, is responsible for the interaction with, and damage of, DNA. Since the experiments were carried out in buffer, the peaks recorded can only be attributed to the reaction of adriamycin molecules that are inside the film of DNA (Fig. **9B**).

Adriamycin reduction clearly conditions the adriamycin-DNA interaction. The adriamycin reactive radical formed interacts with nucleotides inside the DNA helix *in situ* and the products are retained in the DNA layer. These results are in agreement with those obtained with the thick layer DNA-modified GCE [51]. The clear separation of the adriamycin and 8-oxoG peaks is very important as it enables the use of the less positive 8-oxoGua oxidation peak to detect oxidative DNA damage.

7.2. Imatinib

Imatinib (Fig. **10A**) is a relatively small molecule, and one of the most potent *in vitro* and *in vivo* inhibitors of the protein tyrosine kinase, a protein expressed by all patients with chronic myelogenous leukemia, undergoing extensive evaluation of its activity against other types of tumor.

In order to clarify imatinib pharmacokinetics and interaction with DNA, the multi-layer dsDNA-electrochemical biosensor was immersed in an imatinib solution and after incubation the modified electrode was rinsed with deionized water, and transferred to buffer, where a conditioning potential of + 0.90 V, enabling the pre-concentration of imatinib, was applied during 1 min. The conditioning potential of + 0.90 V does not oxidize the immobilized DNA since the oxidation of dGuo (the most easily oxidized DNA nucleotide) only occurs at a higher potential, + 1.01 V, in pH 4.5 solution [53]. Afterwards, the electrode was transferred to buffer were the experiments were carried out, so, the peaks recorded can only be attributed to the reaction of imatinib molecules that are inside the DNA film Fig. (**10B**).

The imatinib molecules attached to the dsDNA film are oxidized, peak 1a, leading to the formation of the imatinib oxidation product, peak 3a, and a new small peak at + 0.45V. It was found that imatinib binds to dsDNA and this interaction leads to modifications in the dsDNA structure, electrochemically recognized through changes of the anodic oxidation peaks of DNA guanosine and adenosine bases. The oxidation of the imatinib oxidation product, peak 3a, is a reversible process, and the peak at + 0.45 V is only detected after reduction of the oxidized imatinib oxidation product.

In fact, the electrons necessary to reduce the oxidized imatinib oxidation product are transferred from the DNA molecules. Using polynucleotides of known sequence, polyguanine and polyadenine, it was proved [53] that the interaction between imatinib and DNA takes place at adenine

enriched segments. In fact, the electrons necessary to reduce the oxidized imatinib oxidation product are transferred from the adenine molecules, and the electron transfer from the adenine moiety in DNA to the oxidized imatinib oxidation product gives rise to reduced imatinib oxidation product and leads to the formation of 2,8-oxoAde, detected at + 0.45 V.

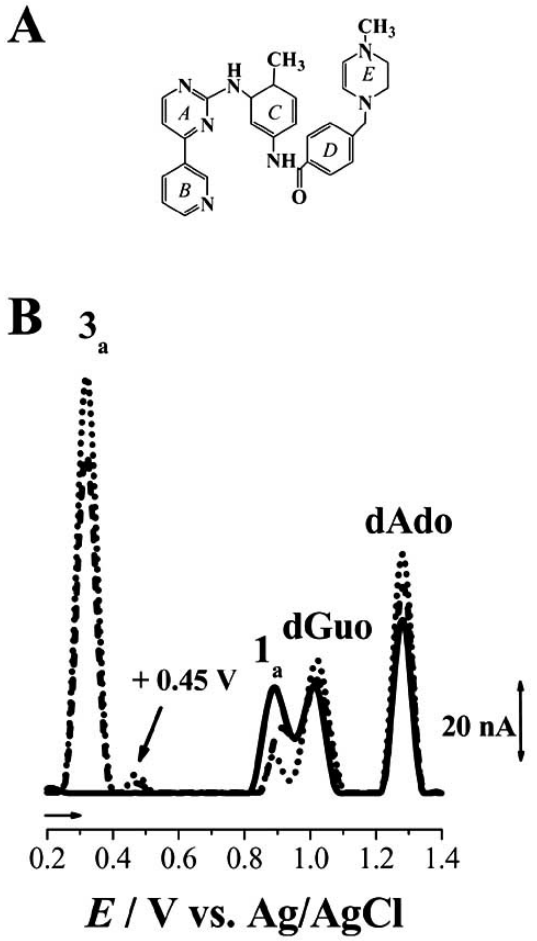

Fig. (10). (**A**) Chemical structure of imatinib and (**B**) baseline corrected differential pulse voltammograms obtained with the dsDNA biosensor in pH 4.5 0.1 M acetate buffer after incubation for 2 minutes with 5 µM imatinib (—) before and after application of 0.90 V during (▪▪▪) 1 and (•••) 2 minutes (from ref. [53] with permission).

The DNA biosensor enabled the pre-concentration of imatinib onto the sensor surface, the *in situ* electrochemical generation of imatinib redox metabolites and the detection of DNA oxidative damage.

7.3. Thalidomide

Thalidomide Fig. (**11A**) is an oral drug marketed in the 1950s as sedative and an anti-emetic during pregnancy that was removed from the market when its teratogenic side effects appeared in new born children. In recent years, thalidomide has regained scientific interest because of its potential for treating a number of otherwise intractable inflammatory skin diseases: erythema nodosum leprosum, a complication of leprosy, graft versus host disease, weight loss in tuberculosis, aphthous ulcers, wasting; and human immunodeficiency virus replication in acquired immune deficiency syndrome and cancer [58, 59].

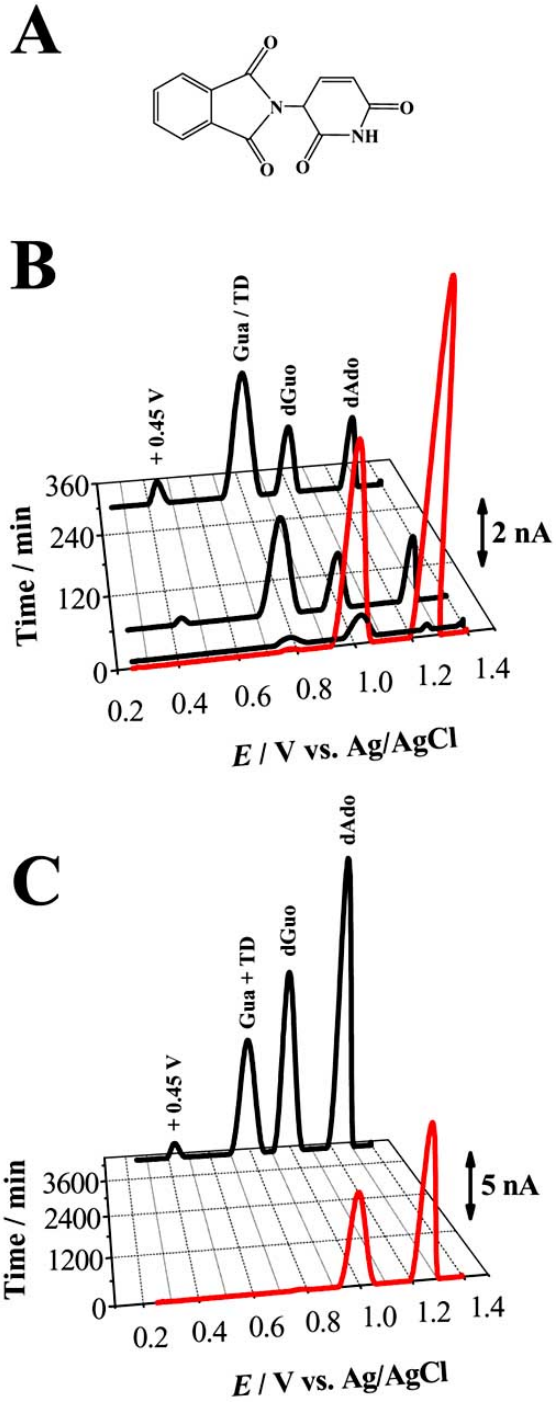

Fig. (11). (**A**) Chemical structure of thalidomide and (**B**, **C**) baseline corrected differential pulse voltammograms of (—) control 100 µg/mL dsDNA and (—) incubated solutions in pH 4.5 0.1 M acetate buffer of: (**B**) 100 µg/mL dsDNA with ~ 40 µM TD during 10 min, 1 h, 5 h and 24 h, and (**C**) 100 µg/mL dsDNA with ~ 40 µM TD during 72 h (from ref. [58] with permission).

Concerning thalidomide teratogenicity, one of the proposed mechanisms considers intercalation into dsDNA, a stacked complex being formed between the flat double phthalimide rings of thalidomide and deoxyguanosine. In solution thalidomide interacts with purines but not with

pyrimidines, with a greater affinity for guanine than for adenine [60].

Different concentrations of thalidomide were incubated for different periods of time with dsDNA and their interaction with dsDNA was studied using AFM, differential pulse voltammetry, UV-Vis and electrophoresis, and the results demonstrated that thalidomide interacts specifically with the dsDNA by intercalation, inducing structural changes in B-DNA, in a time-dependent manner [58]. After 10 min incubation time, thalidomide intercalates into the double-stranded rigid form of DNA and also induce condensation, confirmed by the disappearance of the dGuo and dAdo oxidation peaks (Fig. **11B**).

The intercalation, with the formation of a stacked complex between the flat double phthalimide rings of thalidomide and dGuo, was previously described in the literature [60]. This first step of thalidomide-DNA intercalation changes the physical properties of the DNA double helix: the base-pairs unstick vertically to allow the thalidomide intercalation, the sugar-phosphate backbone is distorted and the helical structure is destroyed. Consequently, the thalidomide-DNA intercalation is followed by DNA double helix unwinding, which leaves the DNA bases and the intercalated thalidomide more exposed to the electrode surface, thus facilitating their oxidation. This clarifies the increase of the thalidomide, dGuo and dAdo oxidation peak currents, with increasing incubation time Fig. (**11C**). However, differential pulse voltammograms showed that thalidomide-DNA condensation still occurs after 24 h incubation (Fig. **11C**). The oxidative damage caused to DNA by thalidomide was also detected electrochemically by the appearance of the 8-oxoGua and/or 2,8 oxoAde oxidation peak (Fig. **11B**, **C**). A control solution of dsDNA was prepared in buffer and analyzed after the same periods of time as the thalidomide-dsDNA incubated solutions (Fig. **11B**, **C**). Consequently, the toxic effects of thalidomide caused to dsDNA, i.e. DNA condensation, intercalation followed by DNA double helix unwinding and oxidative damage, were explained following their electrochemical behavior.

8. CONCLUSION

The dsDNA-electrochemical biosensor is a sophisticated tool to study anticancer drugs-DNA interaction, and may contribute to drug discovery and effective treatment for cancer through providing knowledge about the efficacy of new drug binding with DNA and through information on the mechanism of drug-DNA interactions.

The advantage of the dsDNA-electrochemical biosensor in studying the mechanisms of anticancer drug-DNA interaction is that it is a clean chemical system, the great sensitivity offers the possibility to follow the interaction of anticancer drugs with DNA under different conditions and allows pre-concentration of the anticancer drugs investigated onto the sensor surface and *in situ* electrochemical generation of intermediate radical formation and drug metabolites.

The approach described can be used for the understanding of dsDNA interactions with various complex agents and individual chemicals of environmental, food and medical interest. The use of voltammetric inexpensive and fast detection techniques for the *in situ* generation of reactive intermediates is, in a successful way, a complementary tool for the study of biomolecular interaction mechanisms.

The dsDNA-electrochemical biosensor can contribute in a promising way to the understanding of DNA interaction with molecules or ions and the mechanism through which DNA is oxidatively damaged by anticancer drugs, without using animal tests.

ACKNOWLEDGEMENTS

Financial support from Fundação para a Ciência e Tecnologia (FCT), Ph.D. Grant SFRH/BD/27322/2006 (S.C.B. Oliveira), projects PTDC/QUI/65255/2006, PTDC/QUI/098562/2008, COST Action MP0802, POCI (co-financed by the European Community Fund FEDER), and CEMUC-R (Research Unit 285), is gratefully acknowledged.

REFERENCES

[1] Larsen, I.K. *A Textbook of Drug Design and Development*, Harwood Academic Press: UK, **1991**.

[2] Perry, M.C. *The Chemotherapy Source Book*, Baltimore: USA, **1996**.

[3] Saenger, W. *Principles of Nucleic Acid Structure*, Springer-Verlag: New York, **1984**.

[4] Chaires, J.B. A thermodynamic signature for drug-DNA binding mode. *Arch. Biochem. Biophys.*, **2006**, *453*, 26-31.

[5] Waring, M.J. DNA Modification and Cancer. *Ann. Rev. Biochem.*, **1981**, *50*, 159-192.

[6] Isao, S. Chemistry of drug-induced DNA lesions. *Tox. Lett.*, **1993**, *67*, 3-15.

[7] Palchaudhuri, R.; Hergenrother, P.J. DNA as a target for anticancer compounds: methods to determine the mode of binding and the mechanism of action. *Curr. Opin. Biotechnol.*, **2007**, *18*, 497-503.

[8] Rauf, S.; Gooding, J.J.; Akhtar, K.; Ghauri, M.A.; Rahman, M.; Anwar, M.A.; Khalid, A.M. Electrochemical approach of anticancer drugs-DNA interaction. *J. Pharmaceut. Biomedic.*, **2005**, *37*, 205-217.

[9] Brett, C.M.A.; Oliveira-brett, A.M.O. In *The Encyclopedia of Electrochemistry*; Bard, A.J.; Stratmann, M., Eds. Wiley-VCH Verlag: Germany, **2003**, vol. *3*, pp. 105-124.

[10] Paleček, E.; Fojta, M.; Jelen, F.; Vetterl, V. In *The Encyclopedia of Electrochemistry*; Bard, A.J.; Stratmann, M., Eds. Wiley-VCH Verlag: Germany, **2002**, Vol. *9*, pp. 365-429.

[11] Fojta, M. In *Perspectives in Bioanalysis*; Palecek, E.; Sheller, F.; Wang, J., Eds.; Elsevier: Amsterdam, **2005**; Vol. *1*, pp. 385-431.

[12] Oliveira-Brett, A.M.; Diculescu, V.C.; Chiorcea-Paquim, A.M.; Serrano, S.H.P. In *Comprehensive Analytical Chemistry*, Alegret, S.; Merkoçi, A., Eds.; Elsevier: Amsterdam, **2007**; Vol. *49*, pp. 413-437.

[13] Brett, A.M.O. In *Encyclopedia of Sensors* Grimes, C.A.; Dickey, E.C.; Pishko, M.V., Eds. American Scientific Publishers: USA, **2006**; Vol. *3*, pp 301-314.

[14] Watson, J.D.; Crick, F.H.C. Molecular structure of nucleic acids - a structure for deoxyribose nucleic acid. *Nature*, **1953**, *171*, 737-738.

[15] O'Connor, T.; Mansy, S.; Bina, M.; McMillin, D.R.; Bruck, M.A.; Tobias, R.S. The pH-dependent structure of calf thymus DNA studied by Raman spectroscopy. *Biophy. Chem.*, **1982**, *15*, 53-64.

[16] Zimmerman, S.B.; Pheiffer, B.H. Does DNA adopt the C form in concentrated salt solutions or in organic solvent/water mixtures? An X-ray diffraction study of DNA fibers immersed in various media. *J. Mol. Biol.*, **1980**, *142*, 315-330.

[17] Langridge, R.; Marvin, D.A.; Seeds, W.E.; Wilson, H.R.; Hooper, C.W.; Wilkins, M.H.F.; Hamilton, L.D. The molecular configuration of deoxyribonucleic acid: II. Molecular models and their fourier transforms. *J. Mol. Biol.*, **1960**, *2*, 38-62.

[18] Misra, V.K.; Honig, B. The electrostatic contribution to the B to Z transition of DNA. *Biochemistry*, **1996**, *35*, 1115-1124.

[19] Dryhurst, G.; Elving, P.J. Electrochemical oxidation-reduction paths for pyrimidine, cytosine, purine and adenine: Correlation and application. *Talanta*, **1969**, *16*, 855-874.

[20] Palecek, E.; Jelen, F.; Hung, M.A.; Lasovsky, J. 445 - Reaction of the purine and pyrimidine derivatives with the electrode mercury. *Bioelectrochem. Bioener.*, **1981**, *8*, 621-631.

[21] Barker, G.C. Electron exchange between mercury and denatured DNA strands. *J. Electroanal. Chem.*, **1986**, *214*, 373-390.

[22] Valenta, P.; Nürnberg, H.W. Electrochemical behavior of natural and biosynthetic polynucleotides at the mercury electrode: Part II. Reduction of denatured DNA at stationary and dropping mercury electrodes. *J. Electroanal. Chem.*, **1974**, *49*, 55-75.

[23] Palecek, E.; Postbieglová, I. Adsorptive stripping voltammetry of biomacromolecules with transfer of the adsorbed layer. *J. Electroanal. Chem.*, **1986**, *214*, 359-371.

[24] Palecek, E. Fifty Years of Nucleic Acid Electrochemistry. *Electroanalysis*, 2**009**, *21*, 239-251.

[25] Dryhurst, G.; Elving, P.J. Electrochemical Oxidation of Adenine - Reaction Products and Mechanisms. *J. Electrochem. Soc.*, **1968**, *115*, 1014-1022.

[26] Dryhurst, G. Adsorption of guanine and guanosine at the pyrolytic graphite electrode: Implications for the determination of guanine in the presence of guanosine. *Anal. Chim. Acta*, **1971**, *57*, 137-149.

[27] Yao, T.; Wasa, T.; Musha, S. Anodic voltammetry of deoxyribonucleic-acid at a glassy carbon electrode. *Bul. Chem. Soc. Japan*, **1978**, *51*, 1235-1236.

[28] Oliveira-Brett, A.M.; Matysik, F.M. Voltammetric and sonovoltammetric studies on the oxidation of thymine and cytosine at a glassy carbon electrode. *J. Electroanal. Chem.*, **1997**, *429*, 95-99.

[29] Oliveira-Brett, A.M.; Matysik, F.M. Sonoelectrochemical studies of guanine and guanosine. *Bioelectrochem. Bioener.*, **1997**, *42*, 111-116.

[30] Oliveira-Brett, A.M.; Piedade, J.A.P.; Silva, L.A.; Diculescu, V.C. Voltammetric determination of all DNA nucleotides. *Anal. Biochem.*, **2004**, *332*, 321-329.

[31] Chiorcea-Paquim, A.M.; Piedade, J.A.P.; Wombacher, R.; Jaschke, A.; Oliveira-Brett, A. M. Atomic force microscopy and anodic voltammetry characterization of a 49-mer Diels-Alderase ribozyme. *Anal. Chem.*, **2006**, *78*, 8256-8264.

[32] Brett, C.M.A.; Oliveira-Brett, A.M.; Serrano, S.H.P. On the adsorption and electrochemical oxidation of DNA at glassy carbon electrodes. *J. Electroanal. Chem.*, **1994**, *366*, 225-231.

[33] Ravera, M.; Bagni, G.; Mascini, M.; Osella, D. DNA-metallodrugs interactions signaled by electrochemical biosensors: An overview. *Bioinorg. Chem. Appl.*, **2007**, *91078*, 1-11.

[34] Oliveira-Brett, A.M.; Chiorcea, A.M. Effect of pH and applied potential on the adsorption of DNA on highly oriented pyrolytic graphite electrodes. Atomic force microscopy surface characterisation. *Electrochem. Commun.*, **2003**, *5*, 178-183.

[35] Chiorcea, A.M.; Oliveira-Brett, A.M. Atomic force microscopy characterization of an electrochemical DNA-biosensor. *Bioelectrochemistry*, **2004**, *63*, 229-232.

[36] Oliveira-Brett, A.M.; Chiorcea, A.M. Atomic force microscopy of DNA immobilized onto a highly oriented pyrolytic graphite electrode surface. *Langmuir*, **2003**, *19*, 3830-3839.

[37] Oliveira-Brett, A.M.; Chiorcea-Paquim, A.M. DNA imaged on a HOPG electrode surface by AFM with controlled potential. *Bioelectrochemistry*, **2005**, *66*, 117-124.

[38] Chiorcea-Paquim, A.M.; Oretskaya, T.S.; Oliveira-Brett, A.M. Adsorption of synthetic homo- and hetero-oligodeoxynucleotides onto highly oriented pyrolytic graphite: Atomic force microscopy characterization. *Biophys. Chem.*, **2006**, *121*, 131-141.

[39] Sowerby, S.J.; Cohn, C.A.; Heckl, W.M.; Holm, N.G. Differential adsorption of nucleic acid bases: Relevance to the origin of life. *Proc. Natl. Acad. Sci. USA*, **2001**, *98*, 820-822.

[40] Halliwell, B.; Gutteridge, J.M.C. Biologically Relevant Metal Ion-Dependent Hydroxyl Radical Generation - an Update. *FEBS Lett.*, **1992**, *307*, 108-112.

[41] Halliwell, B.; Gutteridge, J.M.C. *Free radicals in biology and medicine*, Oxford University: UK, **1999**.

[42] Klungland, A.; Bjelland, S. Oxidative damage to purines in DNA: Role of mammalian Ogg1. *DNA Repair*, **2007**, *6*, 481-488.

[43] Shibutani, S.; Takeshita, M.; Grollman, A.P. Insertion of specific bases during DNA-synthesis past the oxidation-damaged base 8-oxodg. *Nature*, **1991**, *349*, 431-434.

[44] Bjelland, S.; Seeberg, E. Mutagenicity, toxicity and repair of DNA base damage induced by oxidation. *Mutat. Res-Fund. Mol. M.* **2003**, *531*, 37-80.

[45] Kasai, H. Analysis of a form of oxidative DNA damage, 8-hydroxy-2'-deoxyguanosine, as a marker of cellular oxidative stress during carcinogenesis. *Mutat. Res-Rev. Mutat.*, **1997**, *387*, 147-163.

[46] Halliwell, B. Oxygen and nitrogen are pro-carcinogens. Damage to DNA by reactive oxygen, chlorine and nitrogen species: measurement, mechanism and the effects of nutrition. *Mutat. Res-Genet. Tox. En.*, **1999**, *443*, 37-52.

[47] Borish, E.T.; Cosgrove, J.P.; Church, D.F.; Deutsch, W.A.; Pryor, W.A. Cigarette tar causes single-strand breaks in DNA. *Biochem. Bioph. Res. Co.*, **1985**, *133*, 780-786.

[48] Olinski, R.; Gackowski, D.; Foksinski, M.; Rozalski, R.; Roszkowski, K.; Jaruga, P. Oxidative DNA damage: assessment of the role in carcinogenesis, atherosclerosis, and acquired immunodeficiency syndrome. *Free Radical Bio. Med.*, **2002**, *33*, 192-200.

[49] Oliveira-Brett, A.M.; Piedade, J.A.P.; Serrano, S.H.P. Electrochemical oxidation of 8-oxoguanine. *Electroanalysis*, **2000**, *12*, 969-973.

[50] Diculescu, V.C.; Piedade, J.A.P.; Oliveira-Brett, A. M. Electrochemical behavior of 2,8-dihydroxyadenine at a glassy carbon electrode. *Bioelectrochemistry*, **2007**, *70*, 141-146.

[51] Oliveira-Brett, A.M.; Vivan, M.; Fernandes, I.R.; Piedade, J.A.P. Electrochemical detection of *in situ* adriamycin oxidative damage to DNA. *Talanta*, **2002**, *56*, 959-970.

[52] Piedade, J.A.P.; Fernandes, I.R.; Oliveira-Brett, A.M. Electrochemical sensing of DNA-adriamycin interactions. *Bioelectrochemistry*, **2002**, *56*, 81-83.

[53] Diculescu, V.C.; Vivan, M.; Oliveira-Brett, A.M. Voltammetric behavior of antileukemia drug glivec. Part III: *In situ* DNA oxidative damage by the glivec electrochemical metabolite. *Electroanalysis*, **2006**, *18*, 1963-1970.

[54] Oliveira-Brett, A.M.; Macedo, T.R.A.; Raimundo, D.; Marques, M.H.; Serrano, S.H.P. Voltammetric behavior of mitoxantrone at a DNA-biosensor. *Biosens. Bioelectron.*, **1998**, *13*, 861-867.

[55] Oliveira-Brett, A.M.; Serrano, S.H.P.; Macedo, T.A.; Raimundo, D.; Marques, M.H.; LaScalea, M.A. Electrochemical determination of carboplatin in serum using a DNA-modified glassy carbon electrode. *Electroanalysis*, **1996**, *8*, 992-995.

[56] La-Scalea, M.A.; Serrano, S.H.P.; Ferreira, E.I.; Oliveira-Brett, A.M. Voltammetric behavior of benznidazole at a DNA-electrochemical biosensor. *J. Pharmaceut. Biomed.*, **2002**, *29*, 561-568.

[57] Oliveira-Brett, A.M.; Serrano, S.H.P.; La-Scalea, M.A.; Gutz, I.G.R.; Cruz, M.L.; Lester, P. In *Methods in enzymology*, Academic Press, **1999**; Vol. *300*, pp. 314-321.

[58] Oliveira, S.C.B.; Chiorcea-Paquim, A.M.; Ribeiro, S.M.; Melo, A.T.P.; Vivan, M.; Oliveira-Brett, A.M. *In situ* electrochemical and AFM study of thalidomide-DNA interaction. *Bioelectrochemistry*, **2009**, *76*, 201-207.

[59] Oliveira, S.C.B.; Vivan, M.; Oliveira-Brett, A.M. Electrochemical behavior of thalidomide at a glassy carbon electrode. *Electroanalysis*, **2008**, *20*, 2429-2434.

[60] Stephens, T.D.; Bunde, C.J.W.; Fillmore, B.J. Mechanism of action in thalidomide teratogenesis. *Biochem. Pharmacol.*, **2000**, *59*, 1489-1499.

Received: December 4, 2009 **Revised: December 25, 2009** **Accepted: December 27, 2009**